X-Ray jets in coronal holes: 3D numerical simulations and Hinode observations.

Fernando Moreno-Insertis[1]

Klaus Galsgaard[2]

Ignacio Ugarte-Urra[3]

[1]Instituto de Astrofisica de Canarias
[2]Niels Bohr Institute Copenhagen
[3]NRL Washington

Coronal hole jets observed by Hinode

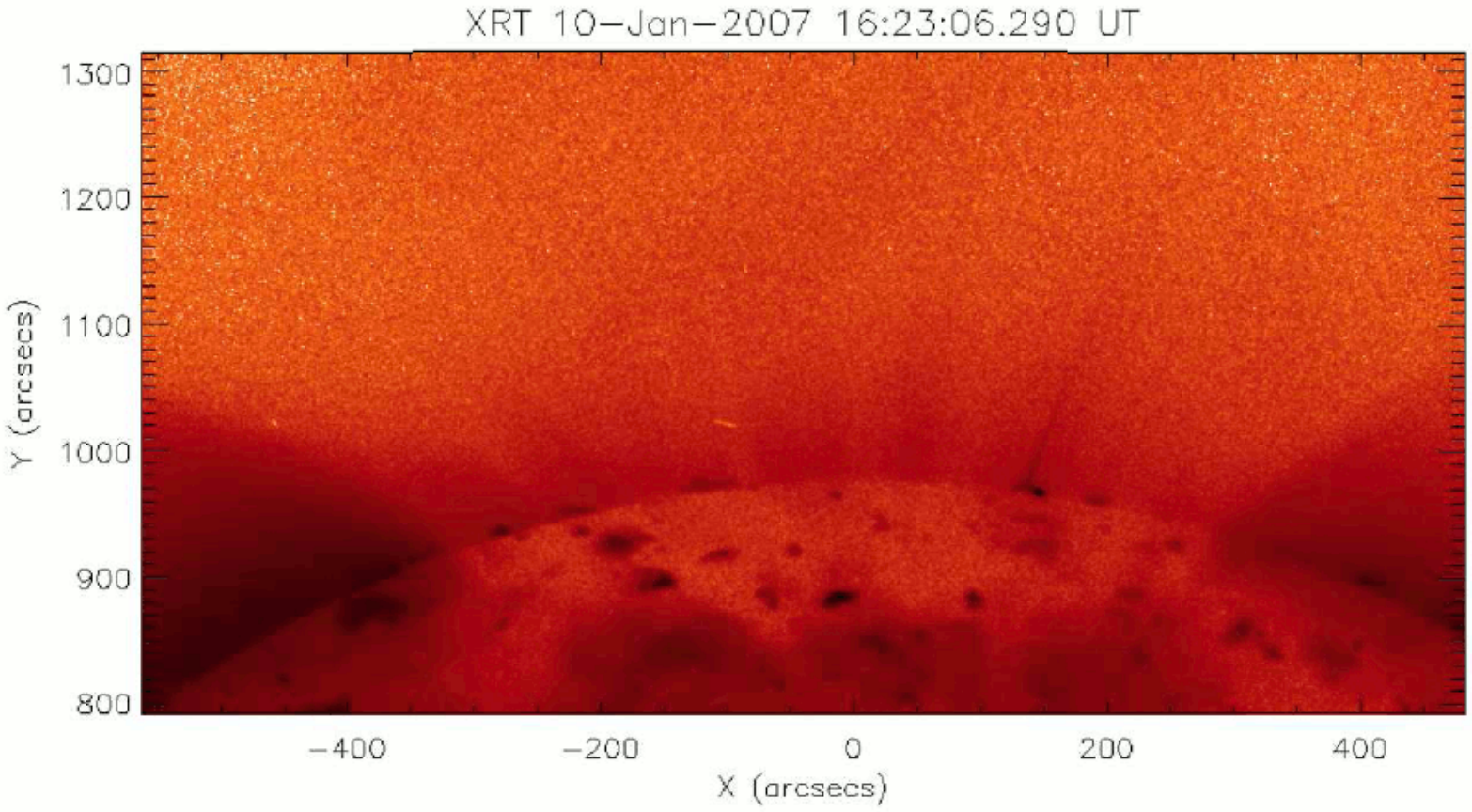

(Cirtain et al 2007)

- Hinode XRT: observation of X-Ray jets in coronal holes

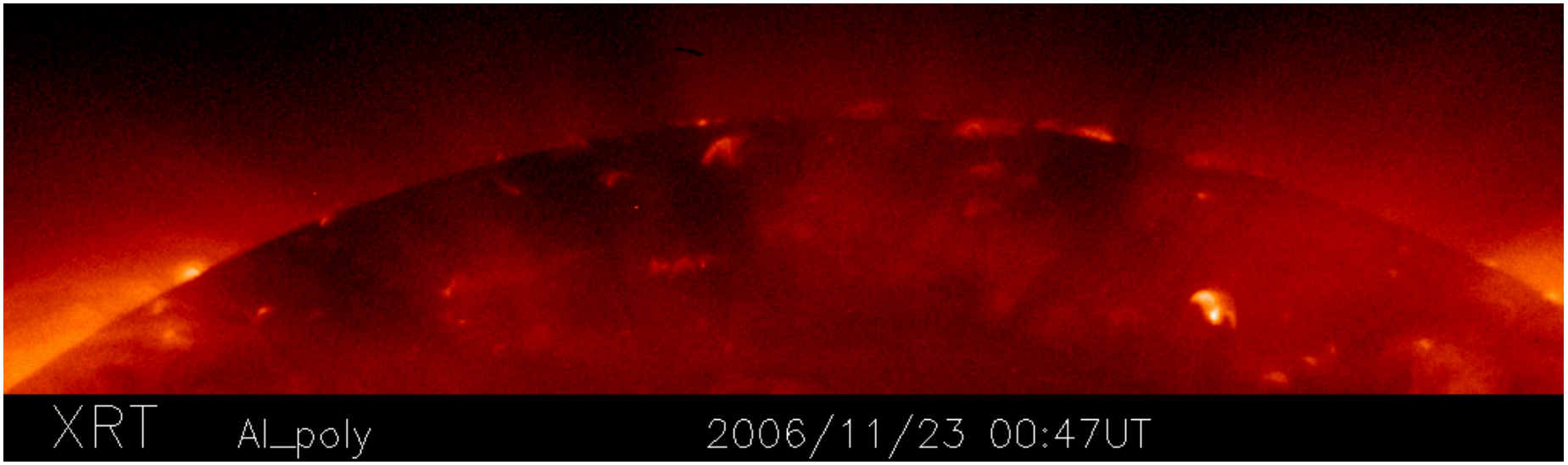

Inverted-Y jet shapes
+ hot coronal loops at the base

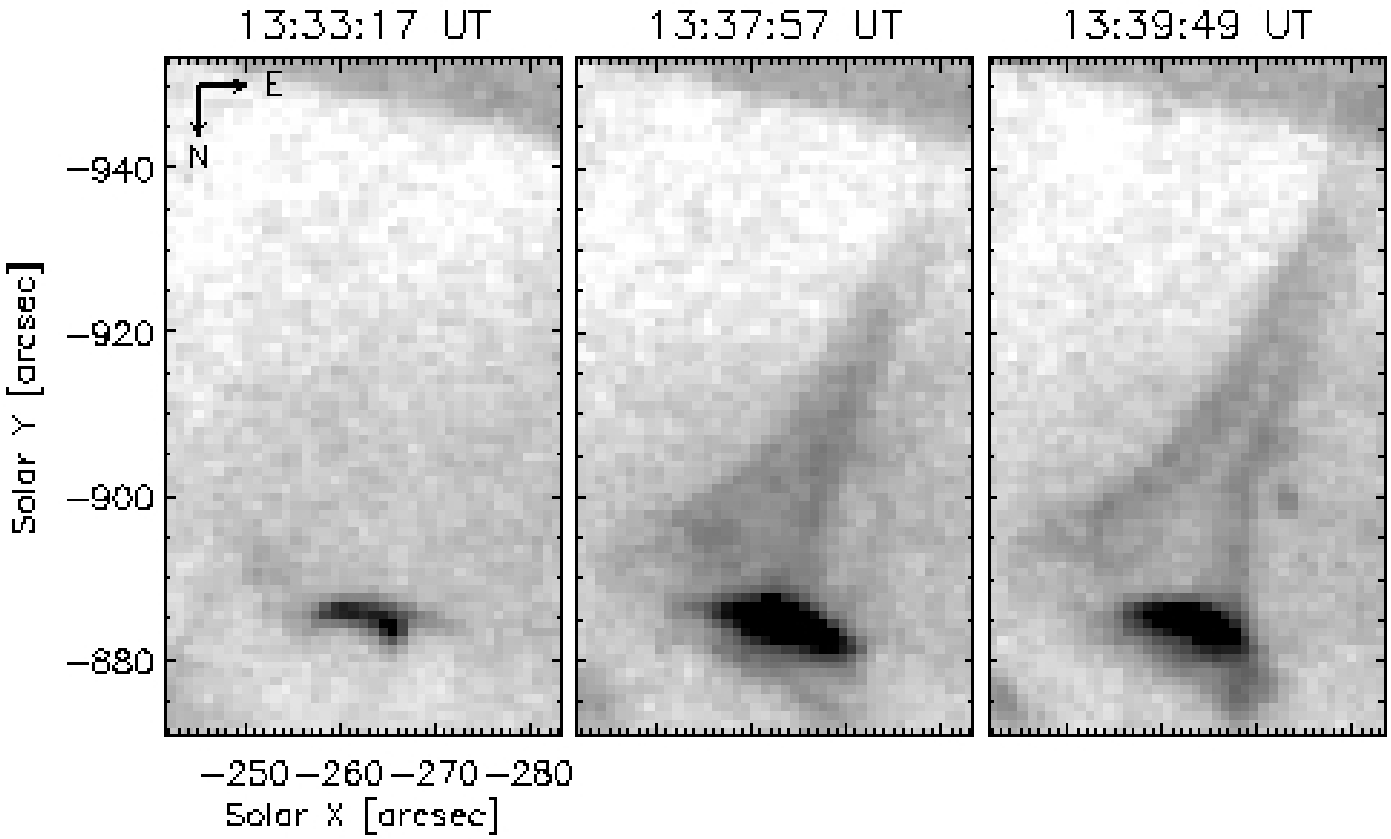

(XRT, Al_poly/open filters, 2007.01.20)

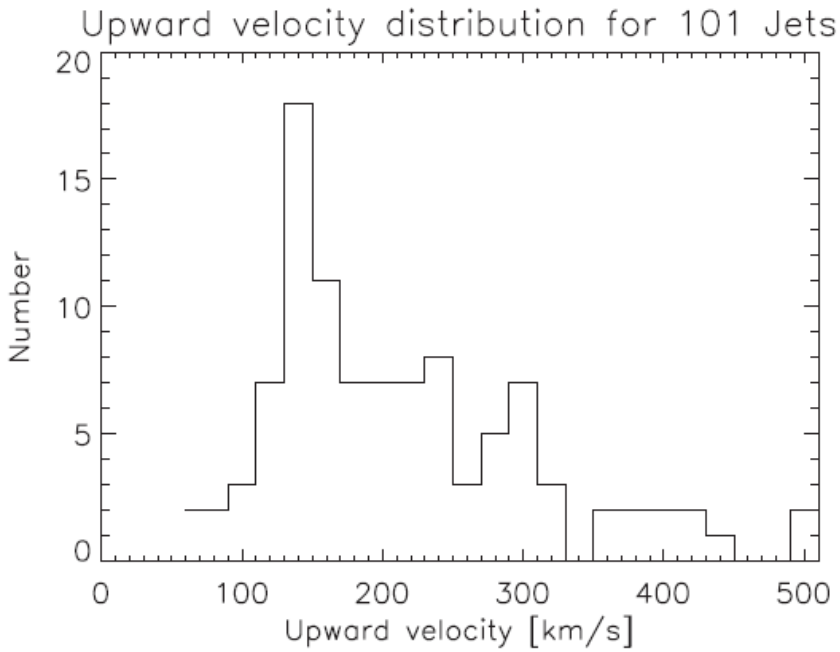

Fig. 4. Histogram distribution of upward jet velocities for 101 jets. Bin size is 20 km s^{-1}.

(Savcheva et al 2007)

Velocity + duration

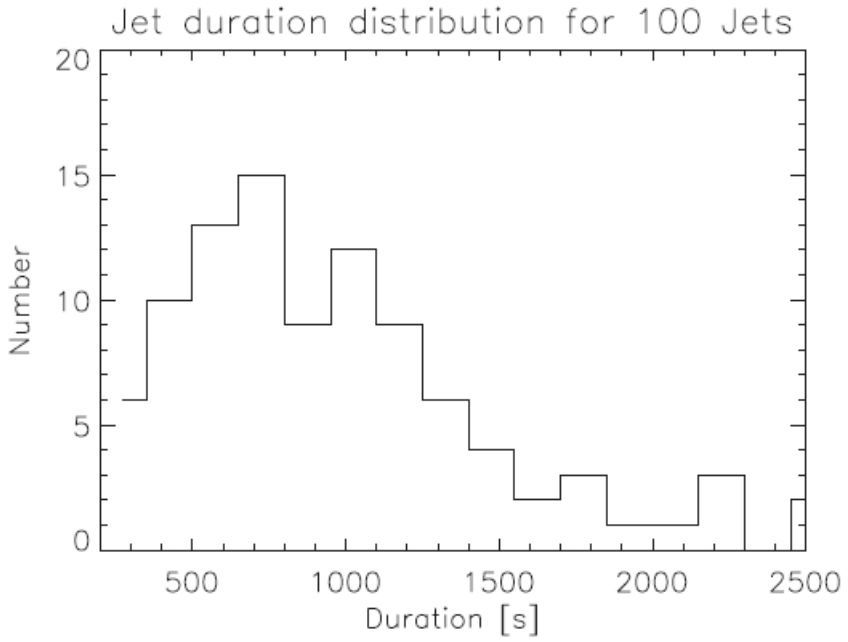

Fig. 8. Histogram distribution of jet durations for 100 jets. The bin size is 150 s.

Observation of a jet in an equatorial coronal hole following flux emergence

Moreno-Insertis, Galsgaard
& Ugarte-Urra, ApJL Feb 08

Simultaneous X-Ray, EUV and magnetogram observations

1) XRT → geometry, location, duration of the jet

2) EIS → jet speeds, electron density

3) SOHO/MDI →full-disk magnetograms →magnetic topology

The jet appeared quasi-simultaneously with a magnetic bipole at the photosphere (10^{19} Mx).

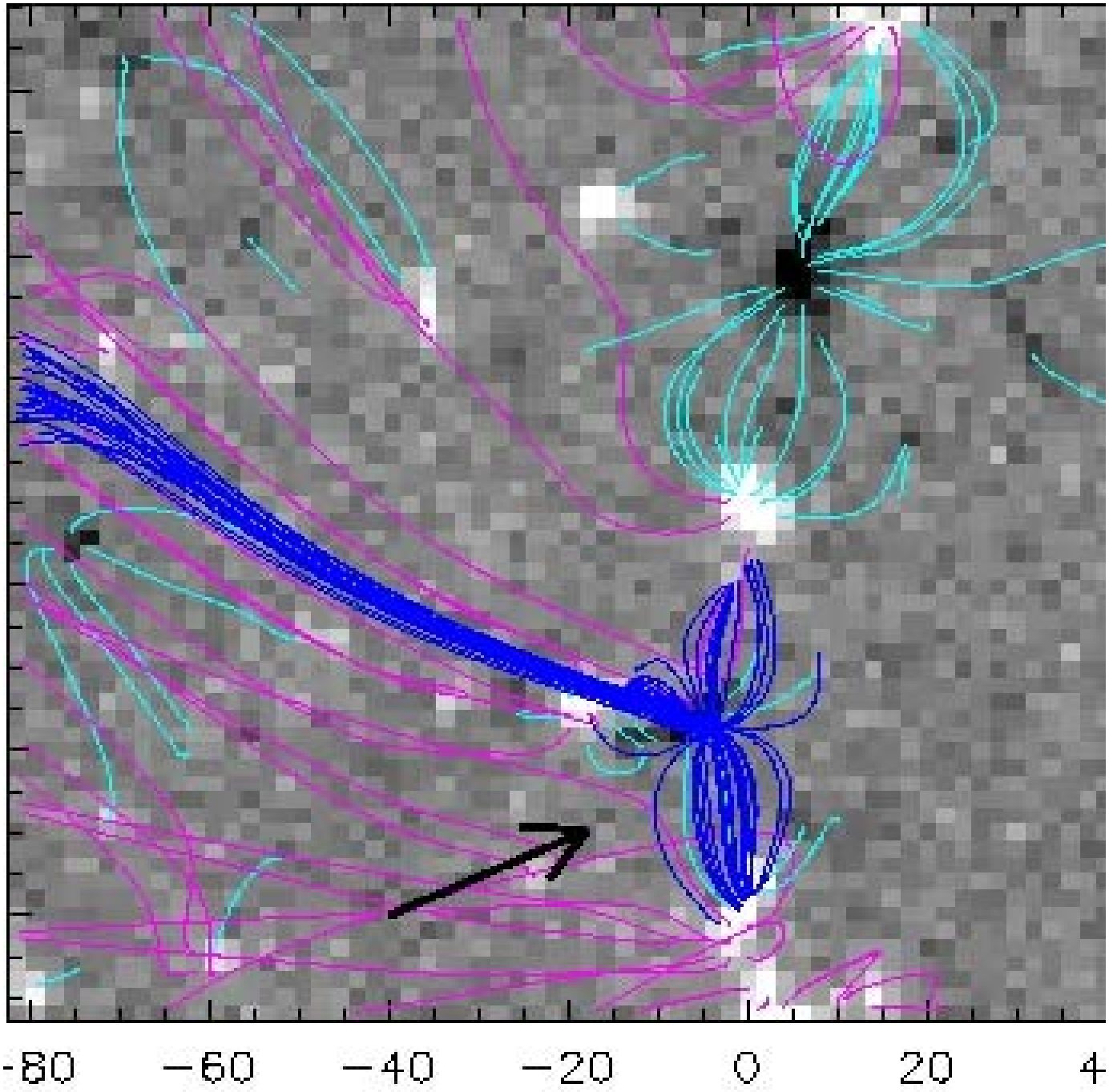
-80
−60
−40
−20
0
20
4

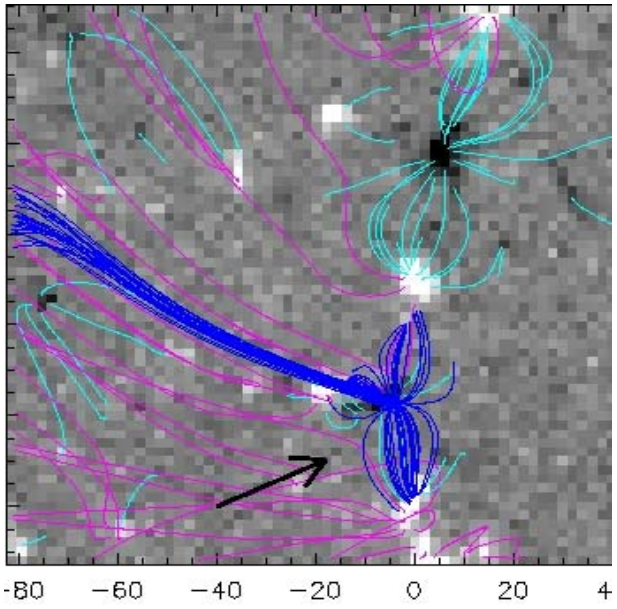
-80
−60
−40
−20
0
20
4

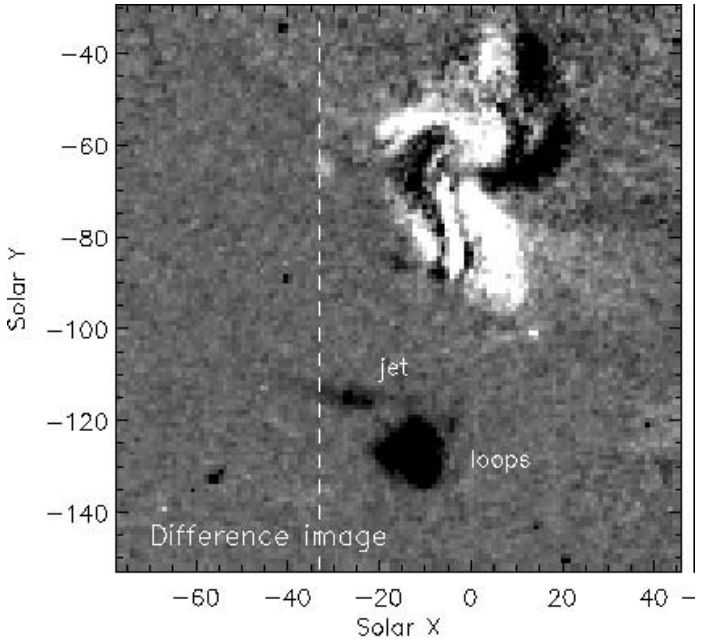
−40
−60
−80
−100
−120
−140
Solar Y
jet
loops
Difference image
−60
−40
−20
0
20
40
Solar X

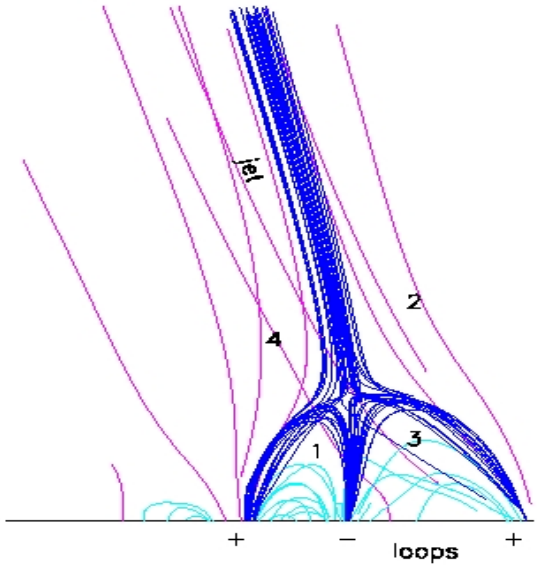
jet
2
4
1
3
+
−
+
loops

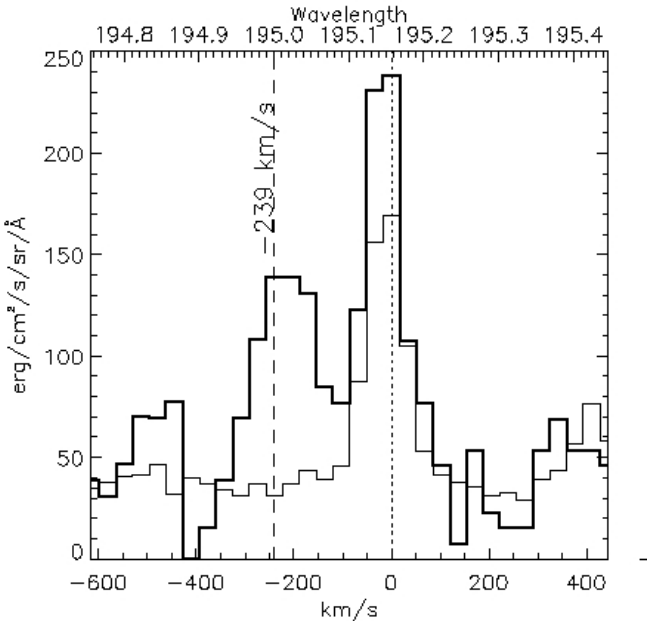
Wavelength
194.8
194.9
195.0
195.1
195.2
195.3
195.4
250
200
150
100
50
0
erg/cm²/s/sr/Å
−239 km/s
−600
−400
−200
0
200
400
km/s

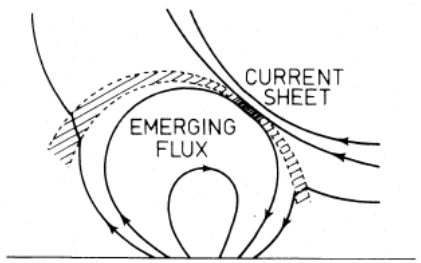

(a) Preflare Heating

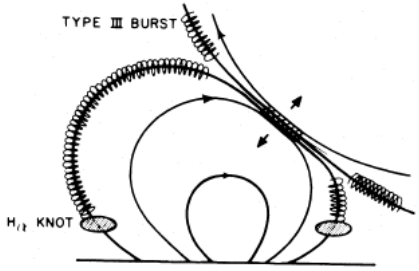

(b) Impulsive Phase

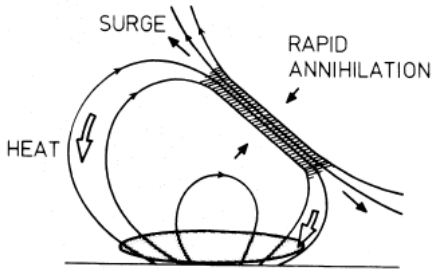

(c) Main Phase

$B_\infty = 0.1$ tesla, the rate of release becomes much larger, namely 0.8×10^{21} W, which may be compared with the 10^{22} W observed to be characteristic of the main phase of a large event. The duration τ_p of the preflare heating is

$$\tau_p = h_{\rm crit}/v_\infty ,$$

where $h_{\rm crit}$ is the altitude attained by the current sheet before the flare is triggered. With $h_{\rm crit} = 10^7$ m and $v_\infty = 10^3$ m s^{-1}, say, we have $\tau_p \approx 20$ minutes.

As the emerging flux pushes higher and higher in the solar atmosphere, eating its way into the overlying field from the photosphere to the lower corona, so the dimensions of the central current sheet change. Its width l and length L are given at each stage by

$$l = \eta/v_\infty , \quad (1)$$

$$L = l v_{A\infty} n_c^{1/2}/(v_\infty n_\infty^{1/2}) , \quad (2)$$

approximately, where $\eta = (\mu_0\sigma)^{-1}$ is the classical Spitzer magnetic diffusivity, n_c is the particle number density inside the current sheet, and

$$\sigma = 1.54 \times 10^{-2} T_c^{3/2}/\log \Lambda \quad \text{mho m}^{-1} \quad (3)$$

is the classical electrical conductivity (Spitzer 1962). Equation (1) follows from a steady balance between convection and diffusion, while equation (2) is a result of mass conservation (Sweet 1958). In addition, the assumption of magnetohydrostatic balance across the sheet (together with the perfect gas law) may be used to write the density ratio as

$$n_c/n_\infty = T_\infty/T_c(1 + \beta_\infty^{-1}) , \quad (4)$$

where

$$\beta_\infty = 3 \times 10^{-29} n_\infty T_\infty B_\infty^{-2}$$

is the ratio of gas to magnetic pressure outside the sheet and has a value of about 10^{-4} for the typical values $B_\infty = 0.01$ tesla, $n_\infty = 10^{16}$ m^{-3}, and $T = 10^5$ K. Also, the electric current density inside the sheet is

$$j = B_\infty(\mu_0 l)^{-1} . \quad (5)$$

FIG. 3.—The emerging flux mechanism for a subflare (or simple loop flare). (*a*), Preflare phase. The emerging flux reconnects with the overlying field. Shock waves (*dashed*) radiate from a small current sheet and heat the plasma as it passes through them into the shaded region. (*b*), Impulsive phase. The onset of turbulence in the current sheet (when it has reached a critical height) causes a rapid expansion. The resulting electric field both in and around the sheet accelerates particles, which then escape along field lines and produce an impulsive microwave burst as they spiral. Those that move downward give rise to hard X-rays and visible flare knots by collisional excitation, while those that escape upward onto open field lines produce type III radio bursts. (*c*), Main phase. The current sheet reaches a new steady state, with reconnection based on a marginally turbulent resistivity. It is much bigger than before, and both heat and particles are conducted down to the lower chromosphere where they produce the Hα flare.

Reconnection and jet emission following flux emergence:

Heyvaerts, Priest & Rust 1977

2D experiment

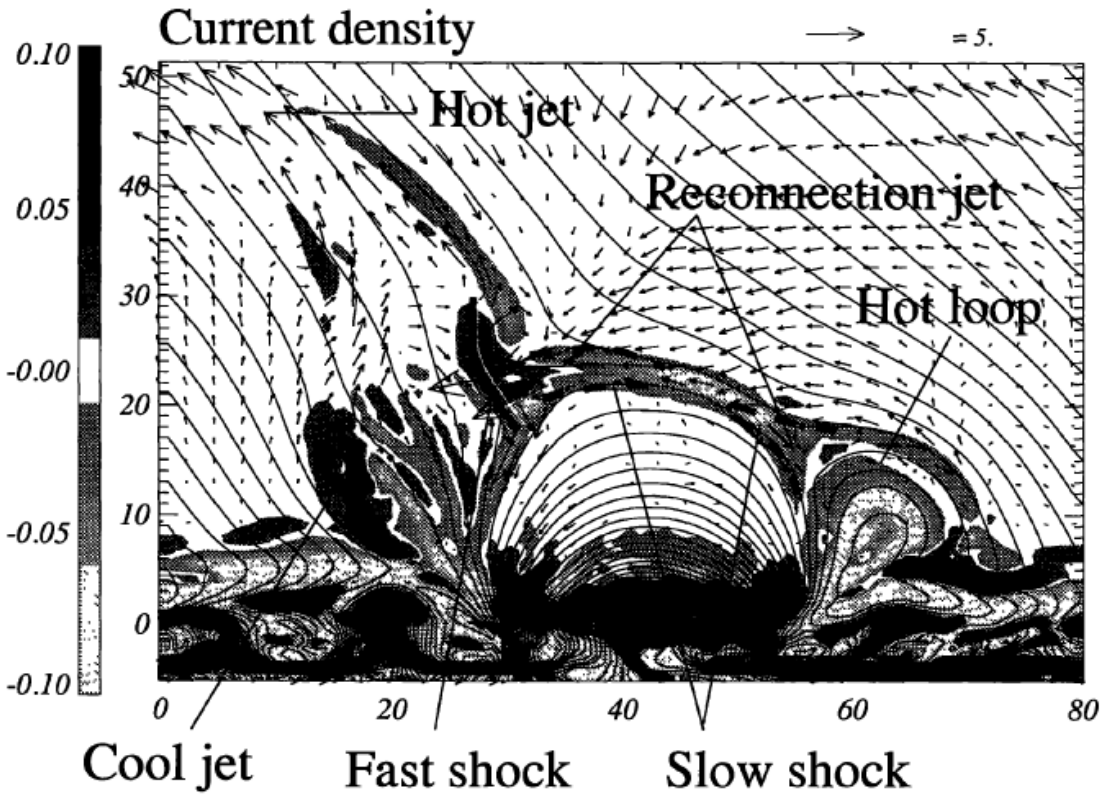

(Shibata et al, PASJ 1992,

Yokoyama & Shibata, PASJ 1996)

3D numerical simulation:

hot jet in a coronal hole following flux emergence

Moreno-Insertis, Galsgaard
& Ugarte-Urra, ApJL Feb 08

The background stratification

- integration domain
  - isothermal corona
  - steep temperature rise (T.R.)
  - isothermal photosphere
  - upper convection zone

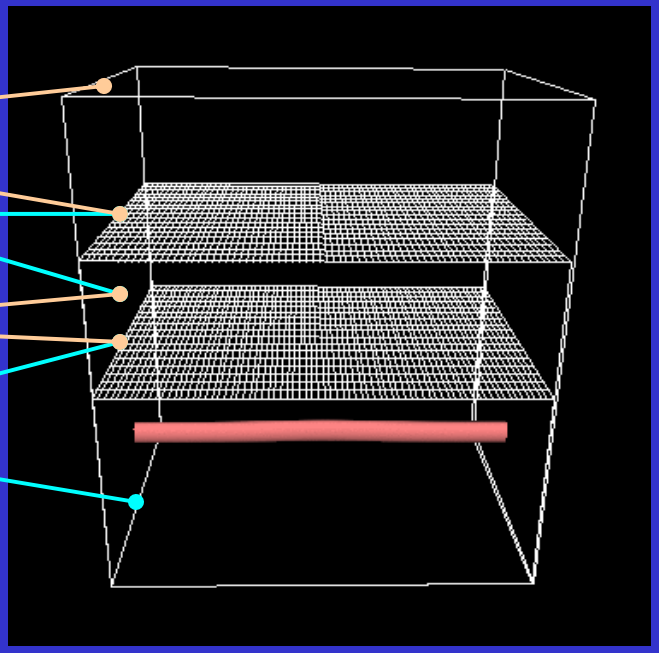

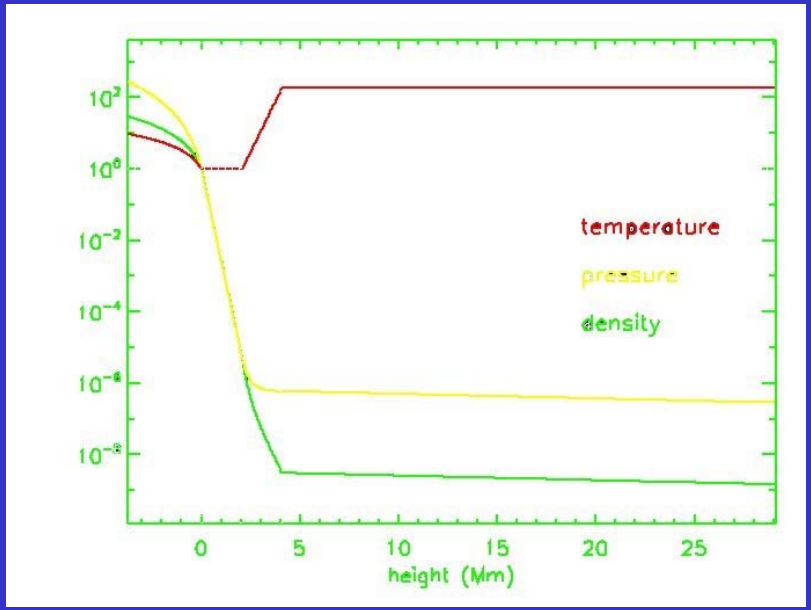

Pressure contrast: 10^9

Density contrast: $2\ 10^{10}$

Background coronal field

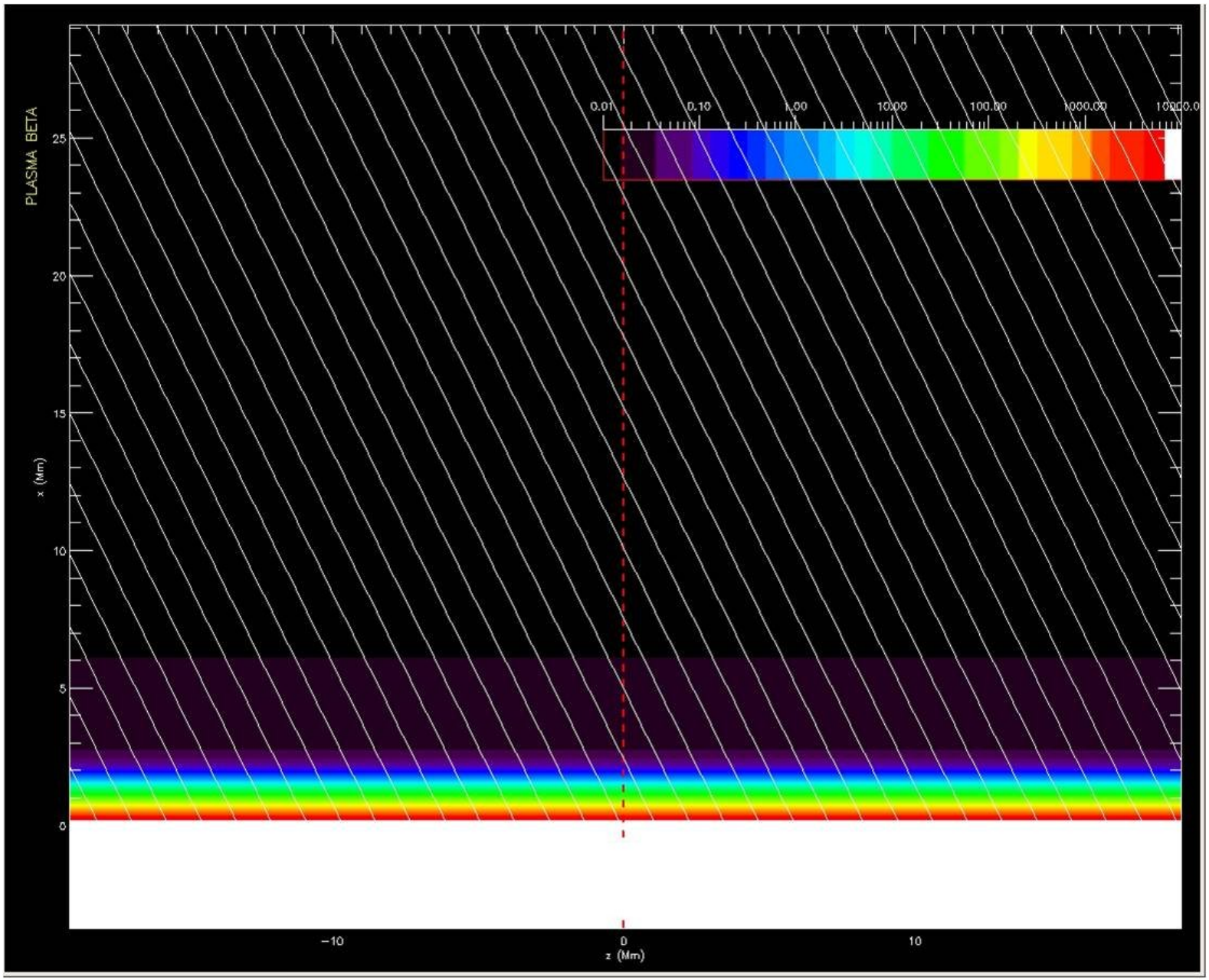

Background coronal field

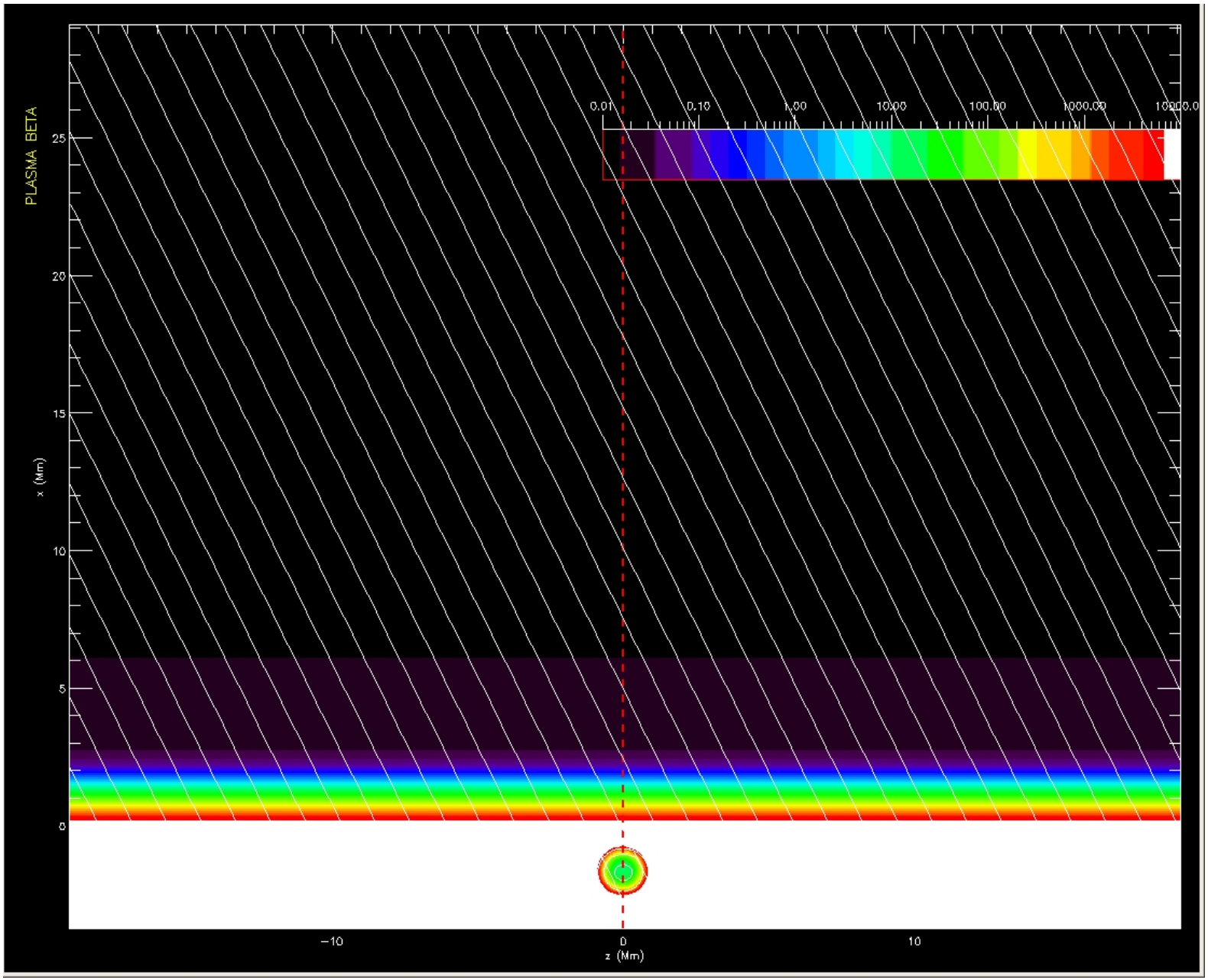

Magnetic field below the surface at time t=0

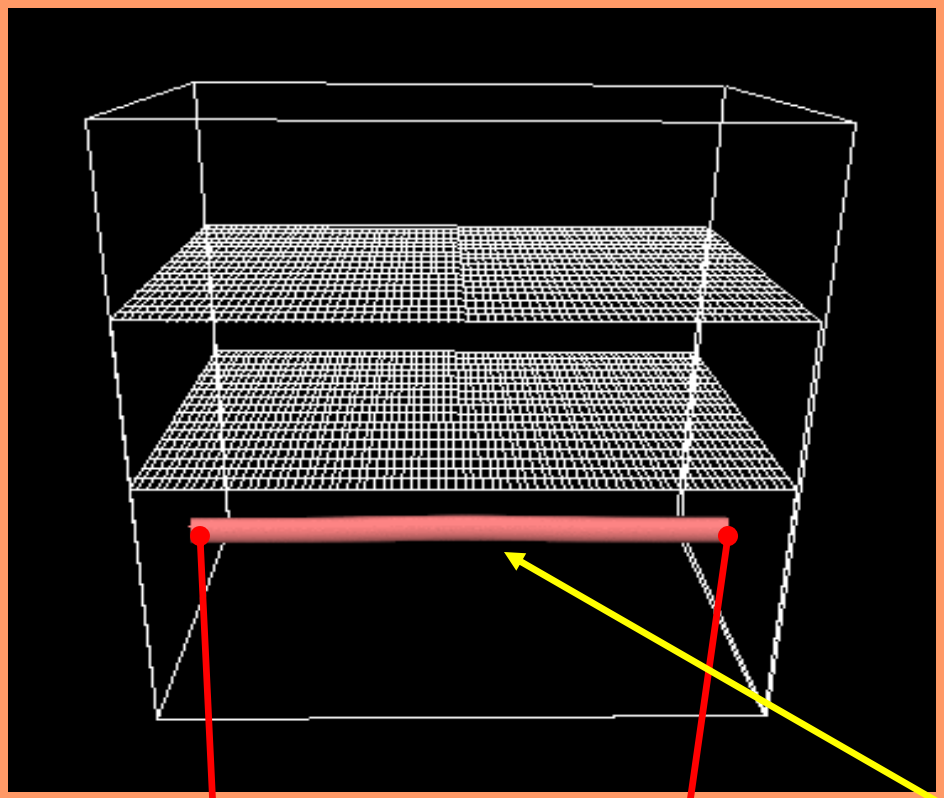

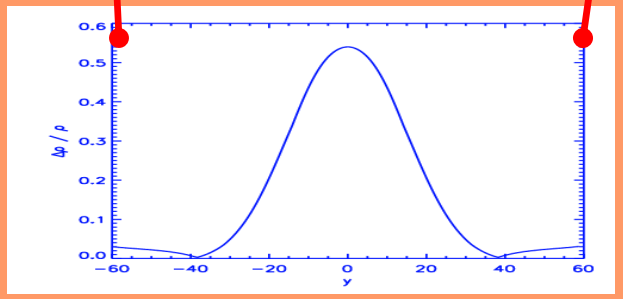

- **equations**: 3D compressible MHD
- **thermodynamics**: ideal gas, no heat conduction, no radiative cooling
- **code**: Nordlund & Galsgaard

- **the field lines are twisted around the tube axis**

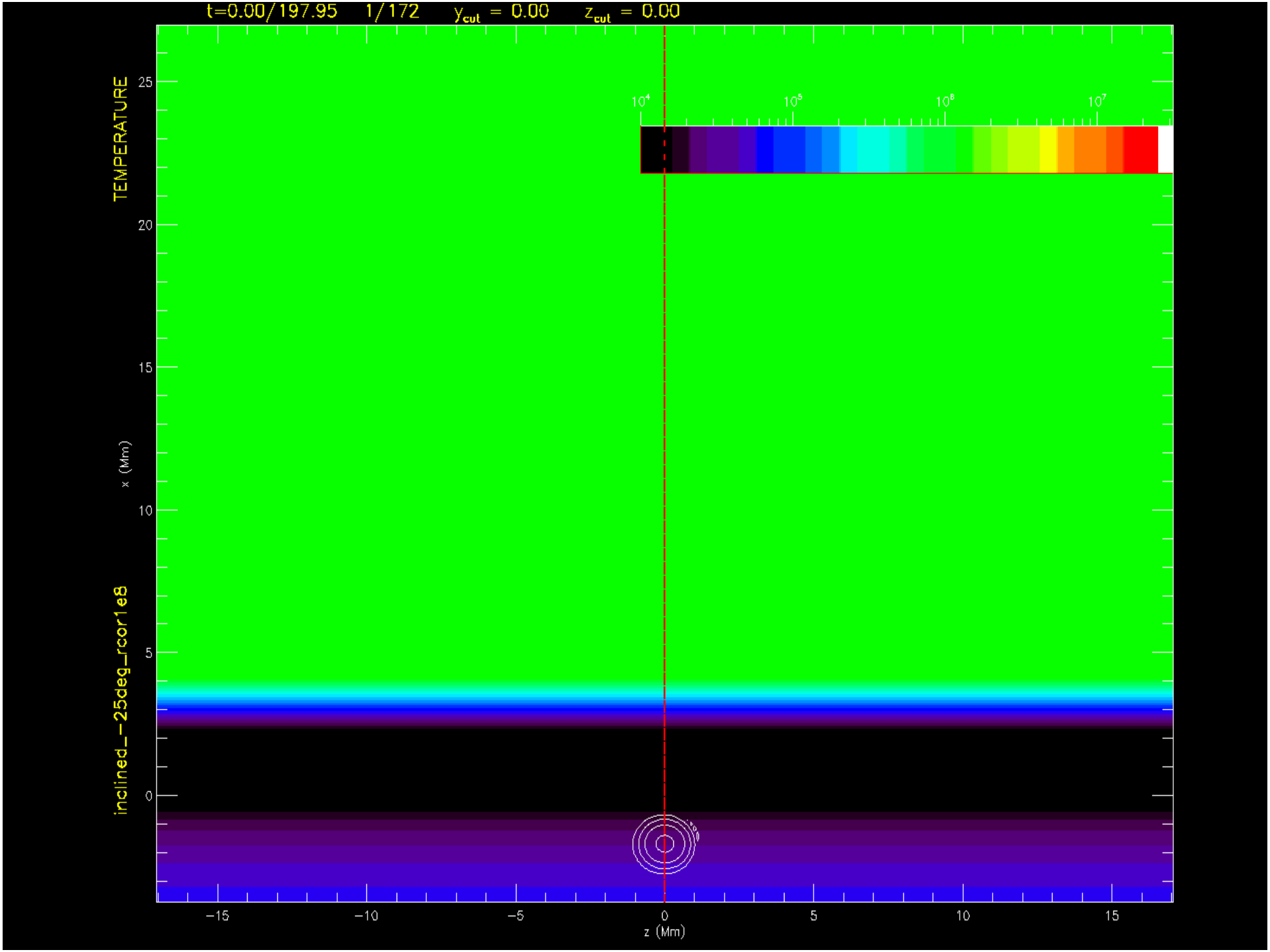
t=0.00/197.95 1/172 y_{cut} = 0.00 z_{cut} = 0.00
TEMPERATURE
10^4
10^5
10^6
10^7
25
20
15
10
5
0
x (Mm)
inclined_-25deg_rcor1e8
−15
−10
−5
0
5
10
15
z (Mm)

Current distribution

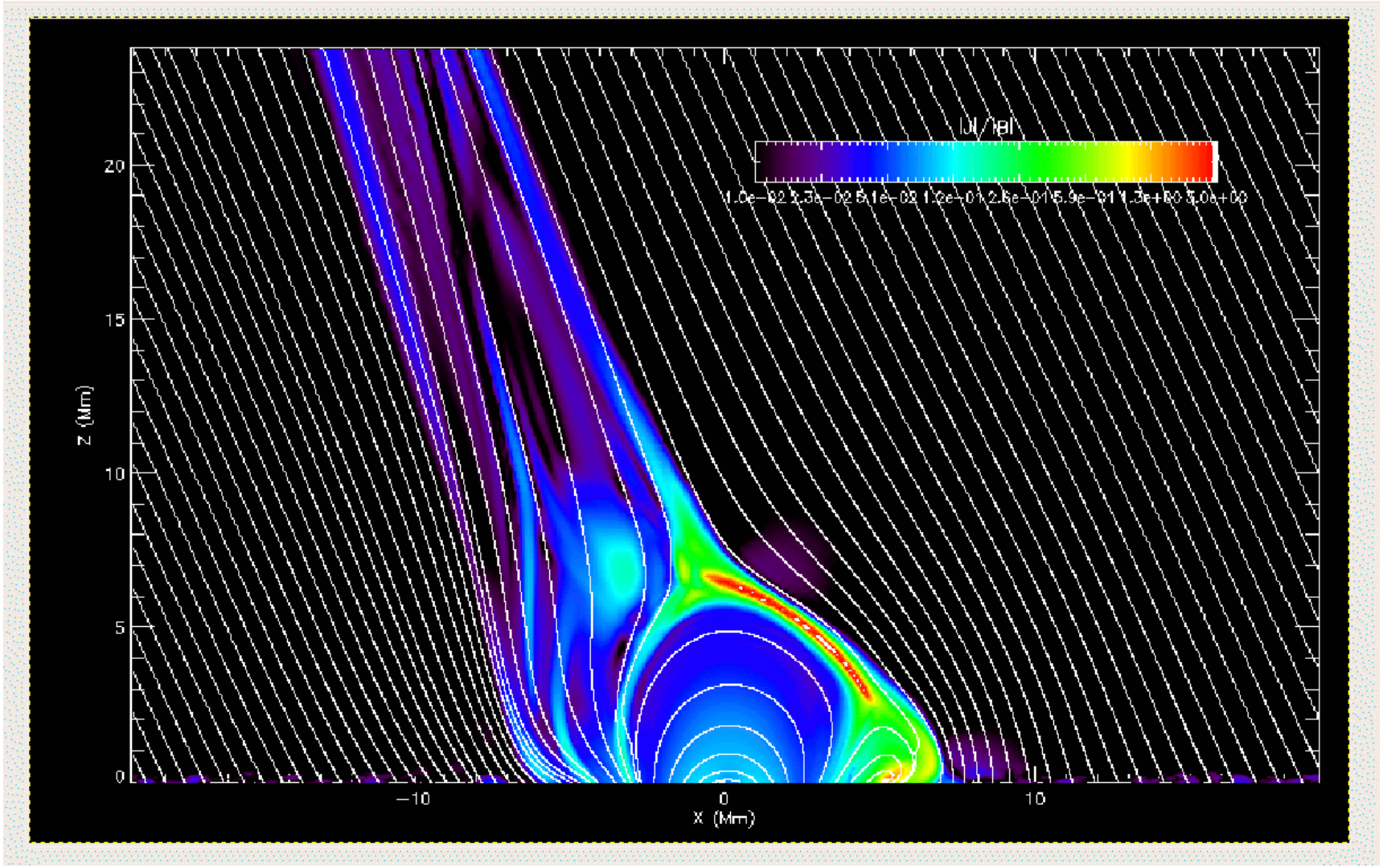

(t=15 min)

Velocity map

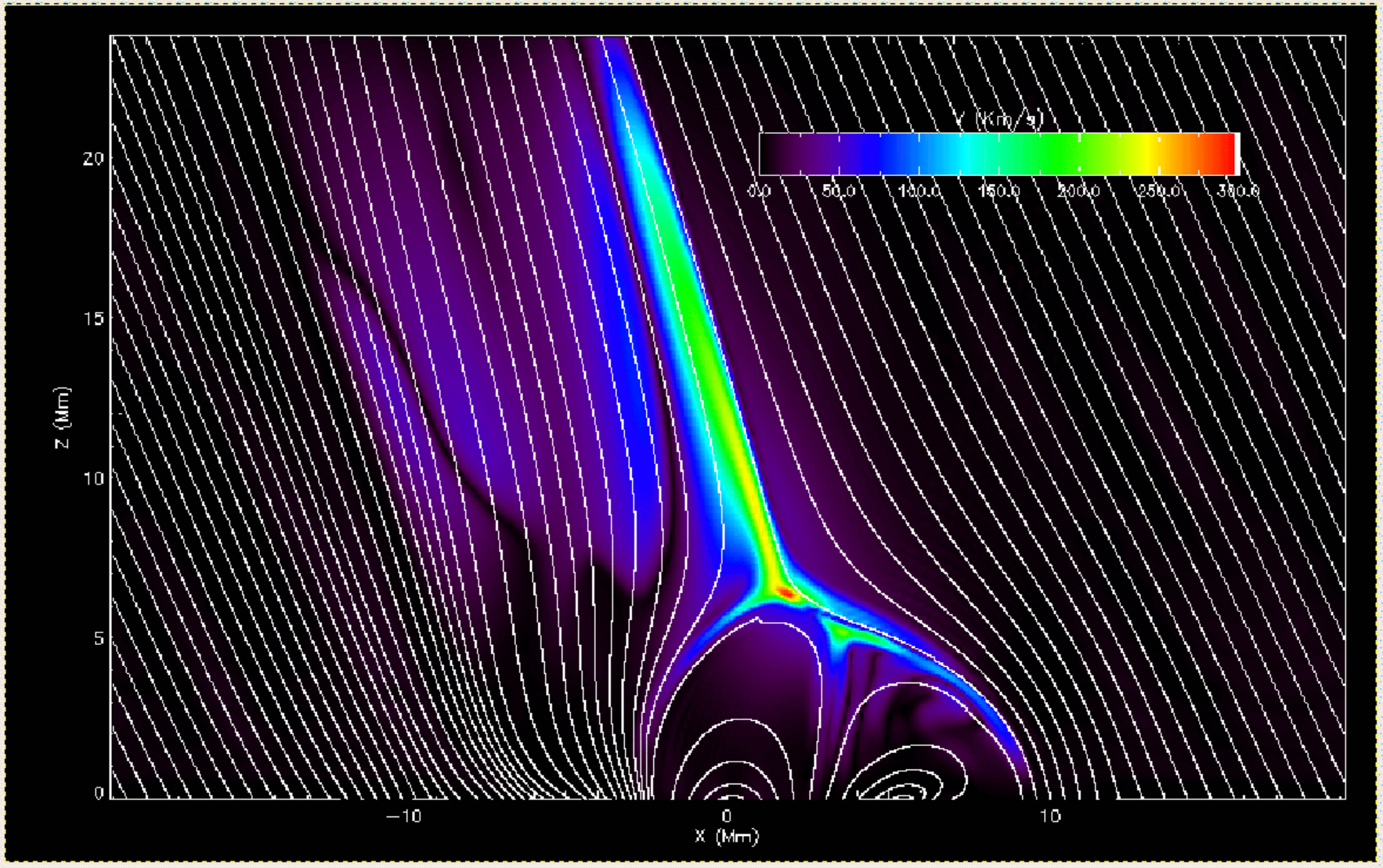

(t=22 min)

3D view: current and temperature

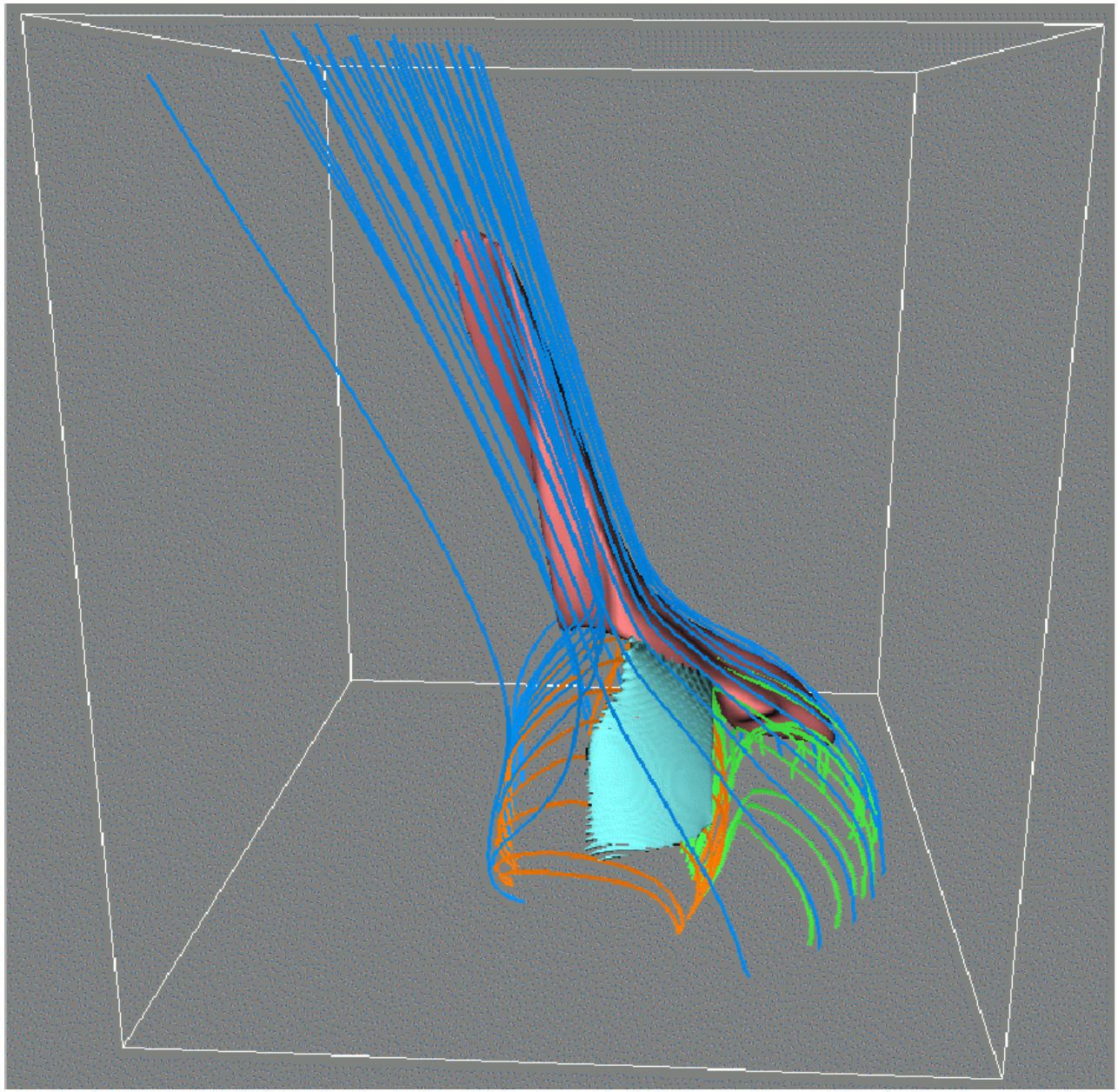

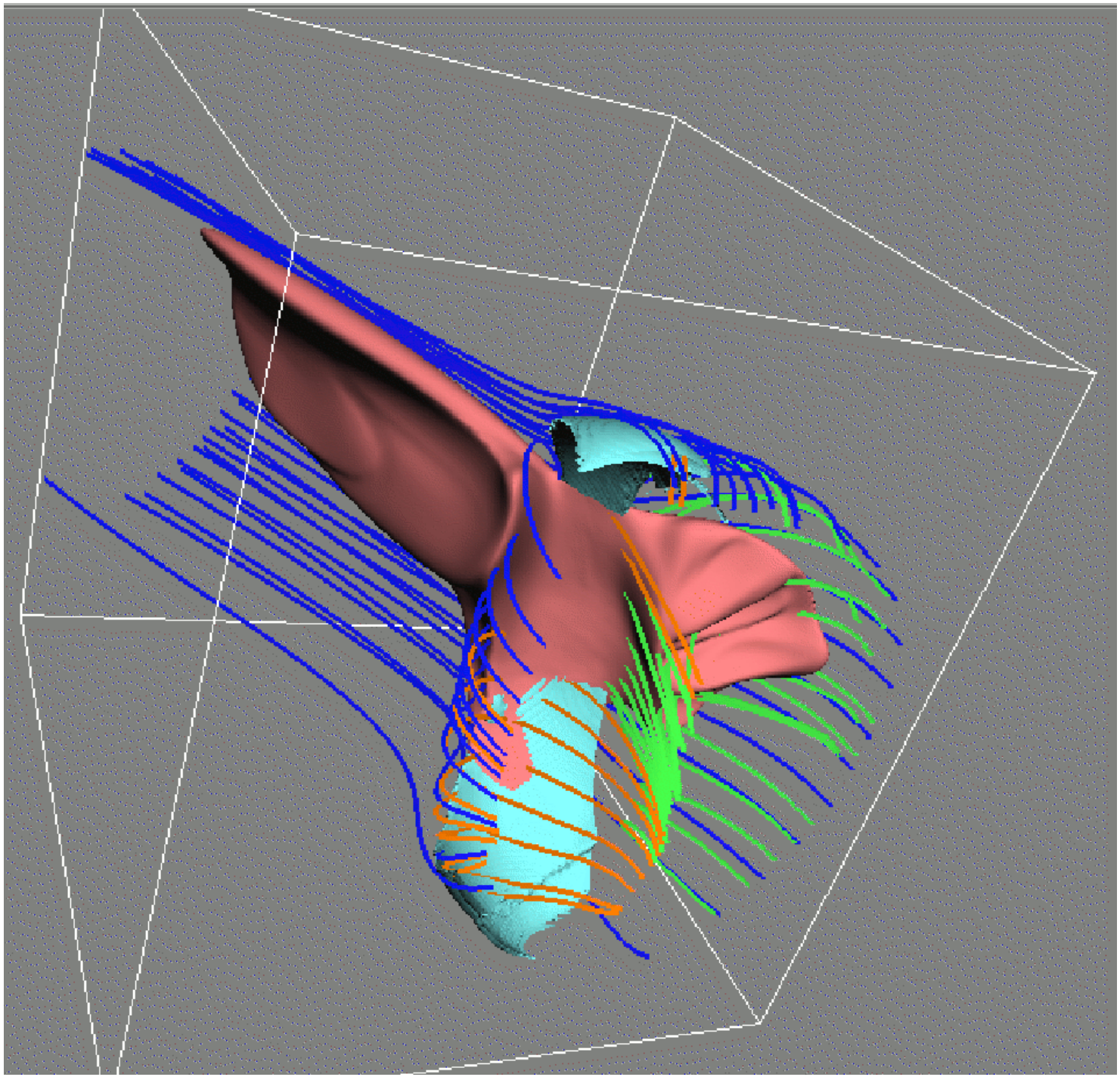

Horizontal drift of the 2-chamber + jet structure

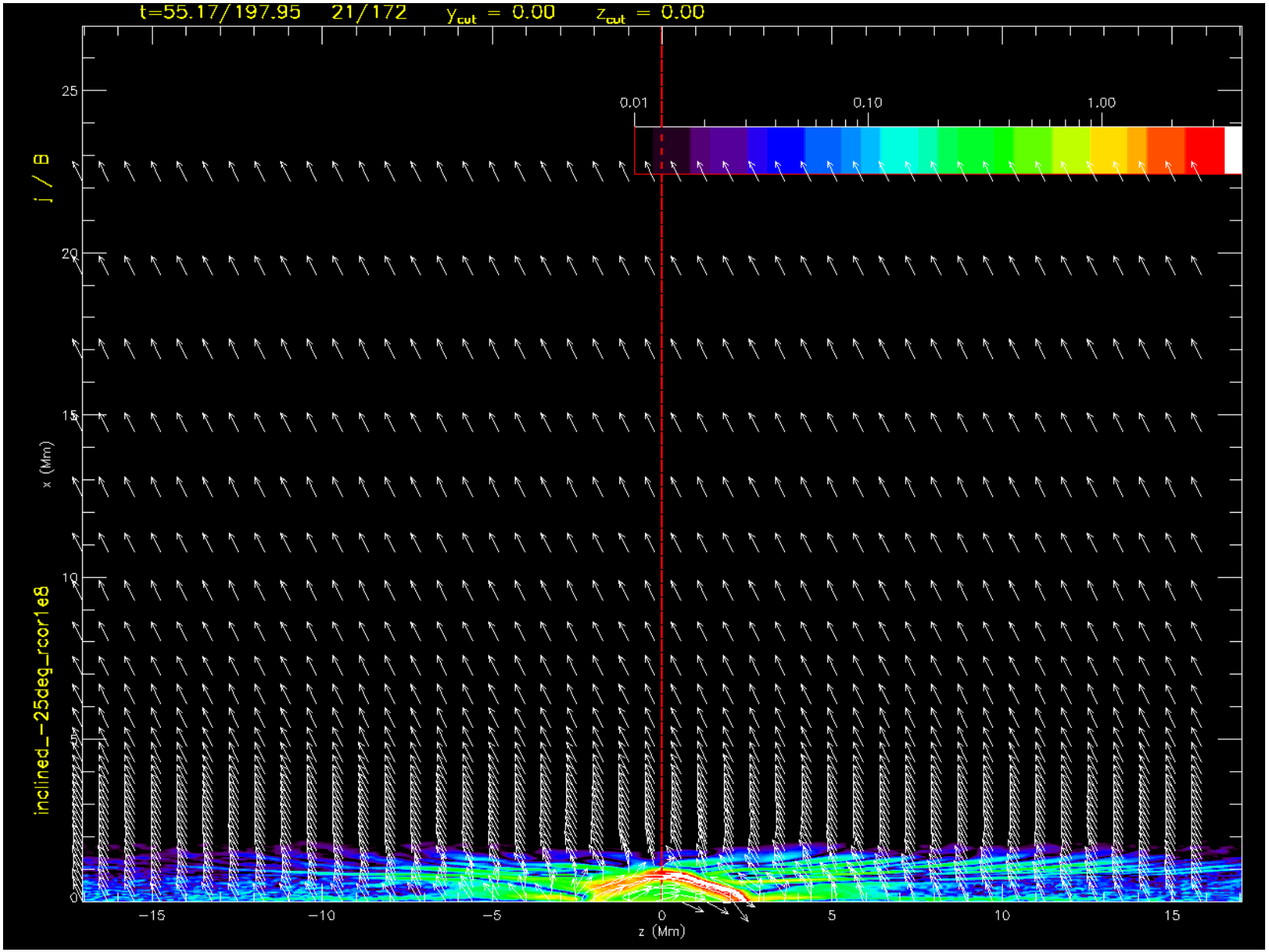

Typical values obtained in the experiment

- **Velocity:**
  - 200 km/s (jet) ------- 400 km/s (reconnection site)
- **Temperature:**
  - 10 MK (jet) -------- 30 MK (reconnection site)
- **Jet duration:** 7 min (main phase) // 22 min (total)
- ***Transverse* velocity**: 10 km / s

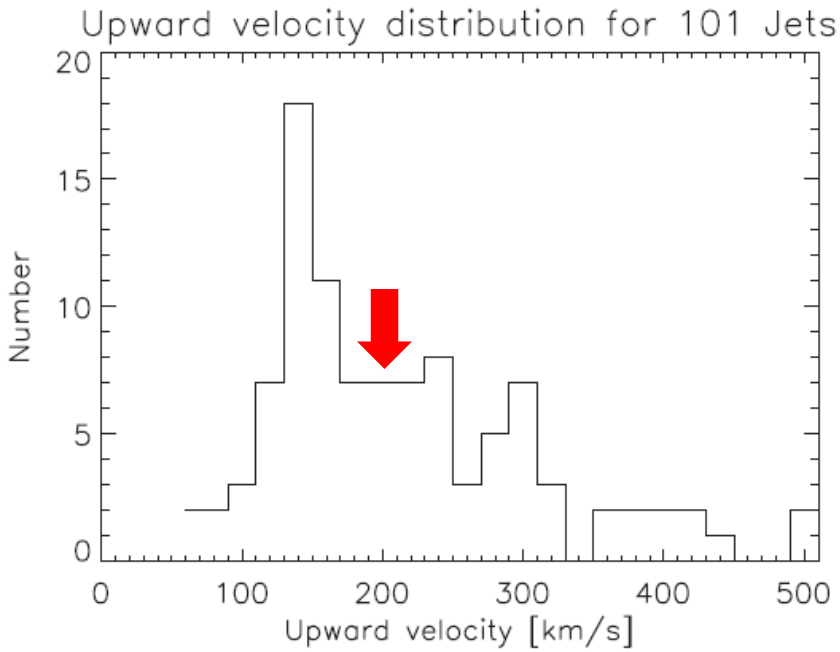

Fig. 4. Histogram distribution of upward jet velocities for 101 jets. Bin size is 20 km s^{-1}.

(Savcheva et al 2007)

Velocity + duration

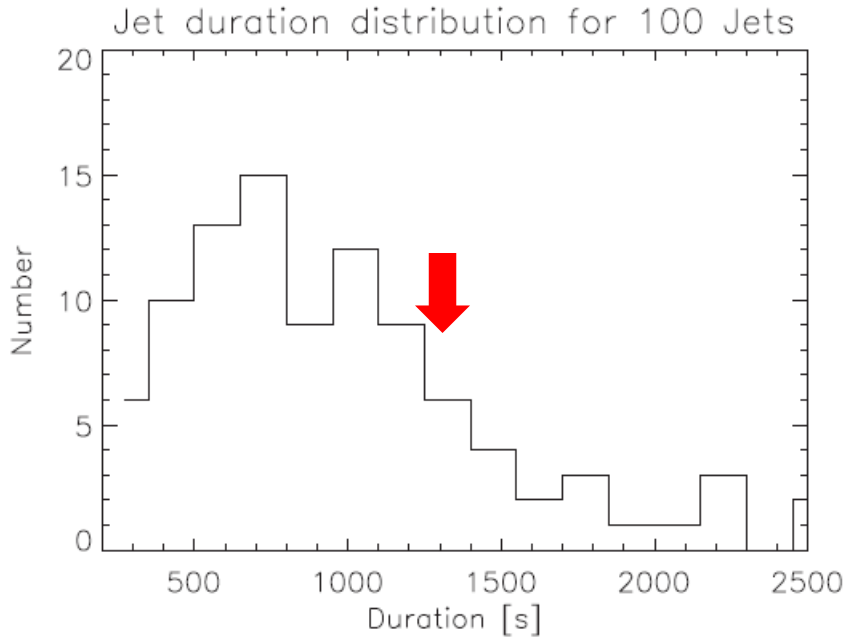

Fig. 8. Histogram distribution of jet durations for 100 jets. The bin size is 150 s.

Drift velocity

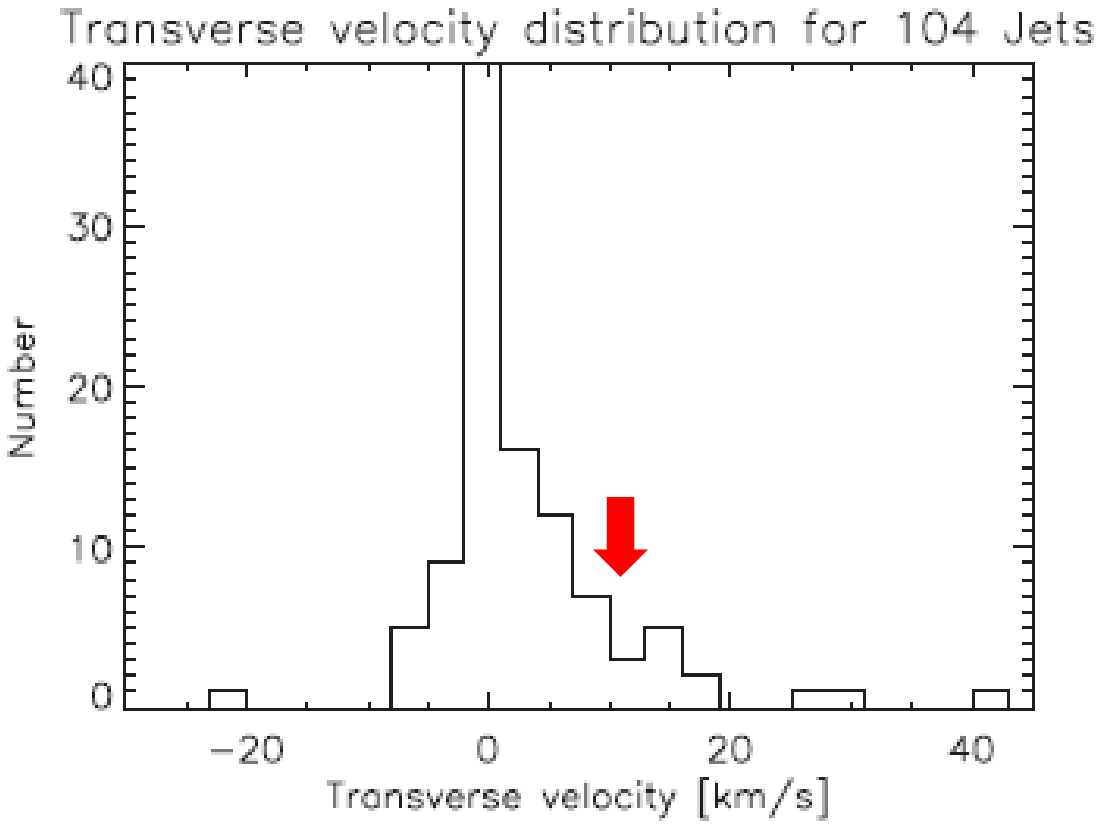

Fig. 7. Histogram distribution of the jet transverse velocities for 104 jets. The bin size is 2 km s^{-1}. The peak at 0 km s^{-1} is artificially high, since the transverse velocities around 0 km s^{-1} of many jets have large uncertainties.

(Savcheva et al 2007)

Some conclusions

- We have studied a jet-formation event with quasi-simultaneous *Hinode* XRT/EIS and *SOHO*/MDI observations.
- A simple force-free extrapolation shows a two-chambered + open field structure
- A 3D flux emergence experiment was done using parameters adequate to a coronal hole.
- The values of temperature, density, velocity, duration and drift speed match approximately those in the Hinode statistical observations.

Temperature map

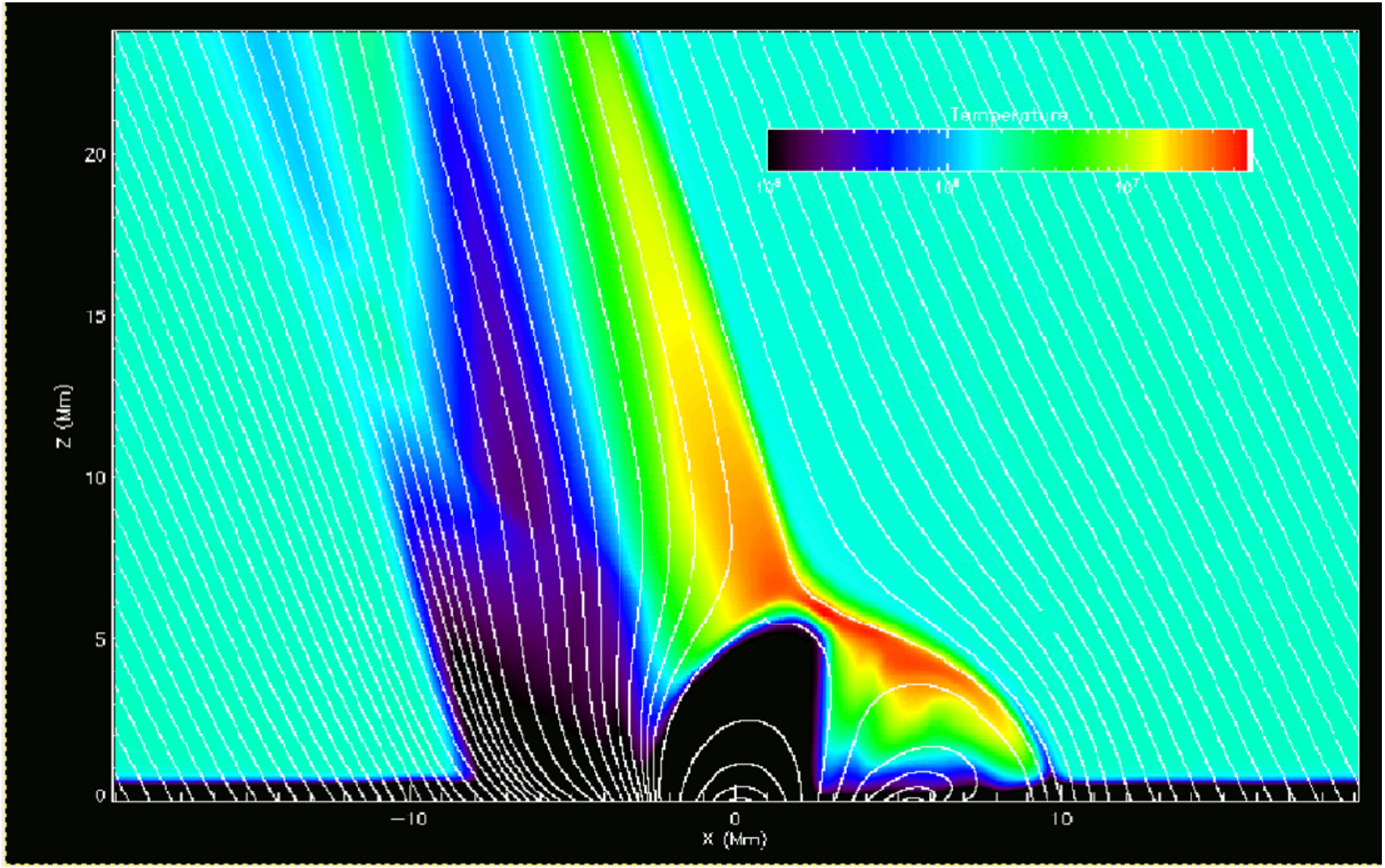

(t=22 min)

- **physical values adequate to a coronal hole were used:**

  $\rightarrow$ $n \approx 2\ 10^8$ atoms cm^{-3}

  $\rightarrow$ open ambient field lines

  $\rightarrow$ coronal field strength: 10 G

  $\rightarrow$ $T \approx 1.1\ 10^6$ K

- **Domain:** 34 Mm x 38 Mm x 33 Mm

  (4 Mm below photosphere,
  29 Mm above photosphere)

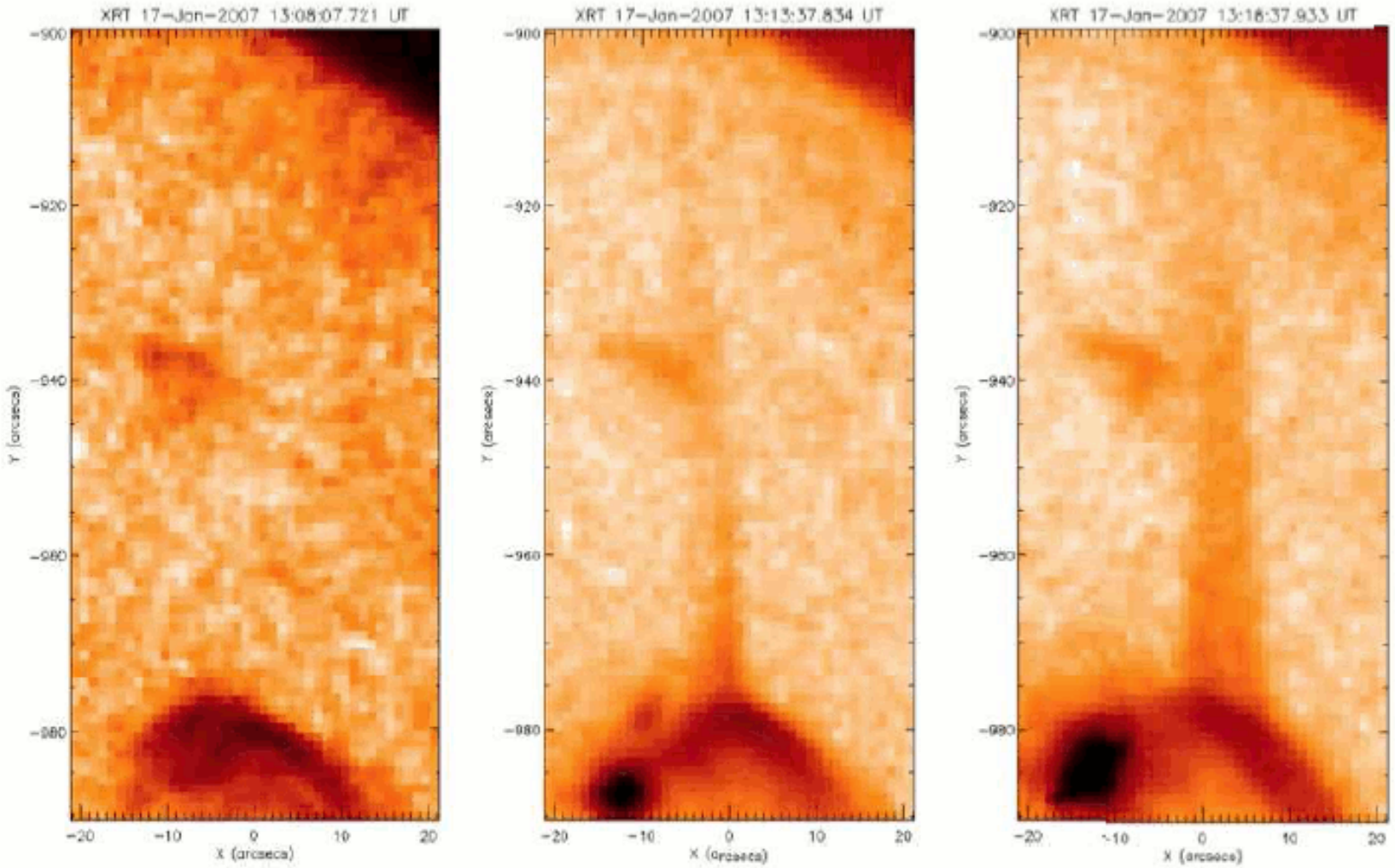

(Cirtain et al 2007)

Figure 2: XRT images of three stages in the jet evolution.

Do the actual values obtained in the experiments fit the Hinode observations?

- **Observations: Savcheva etal 2007**
- **Statistics from 7197 polar jets using Hinode/Soho**

- Jet velocity distribution peaks at 150 km /s
- Jet duration between 8 and 25 min
- *Transverse* (=drift?) velocities between 0 and 20 km / s

=> **the overall agreement is good**

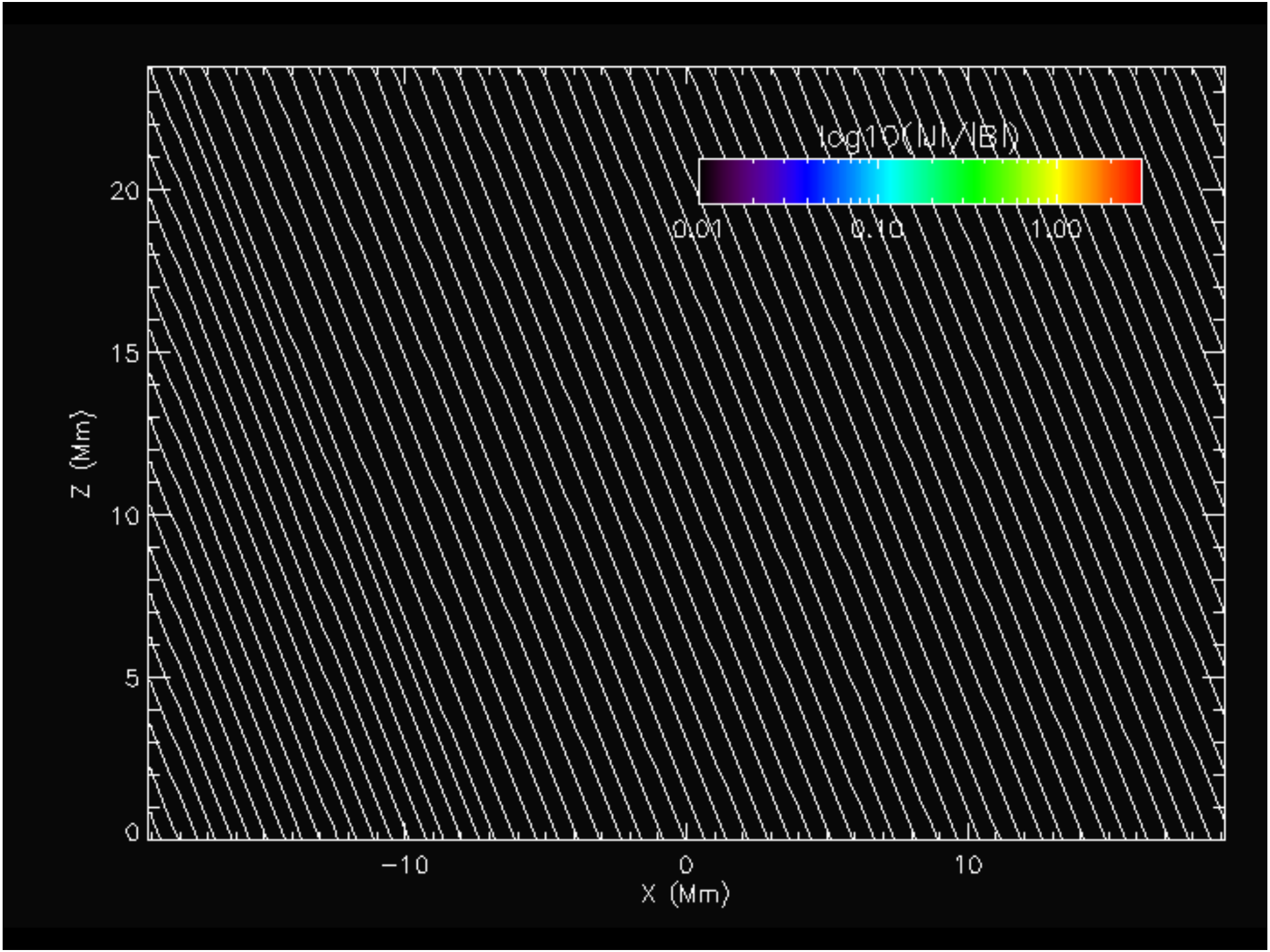
log10(|J|/|B|)
0.01
0.10
1.00
20
15
10
5
0
Z (Mm)
−10
0
10
X (Mm)

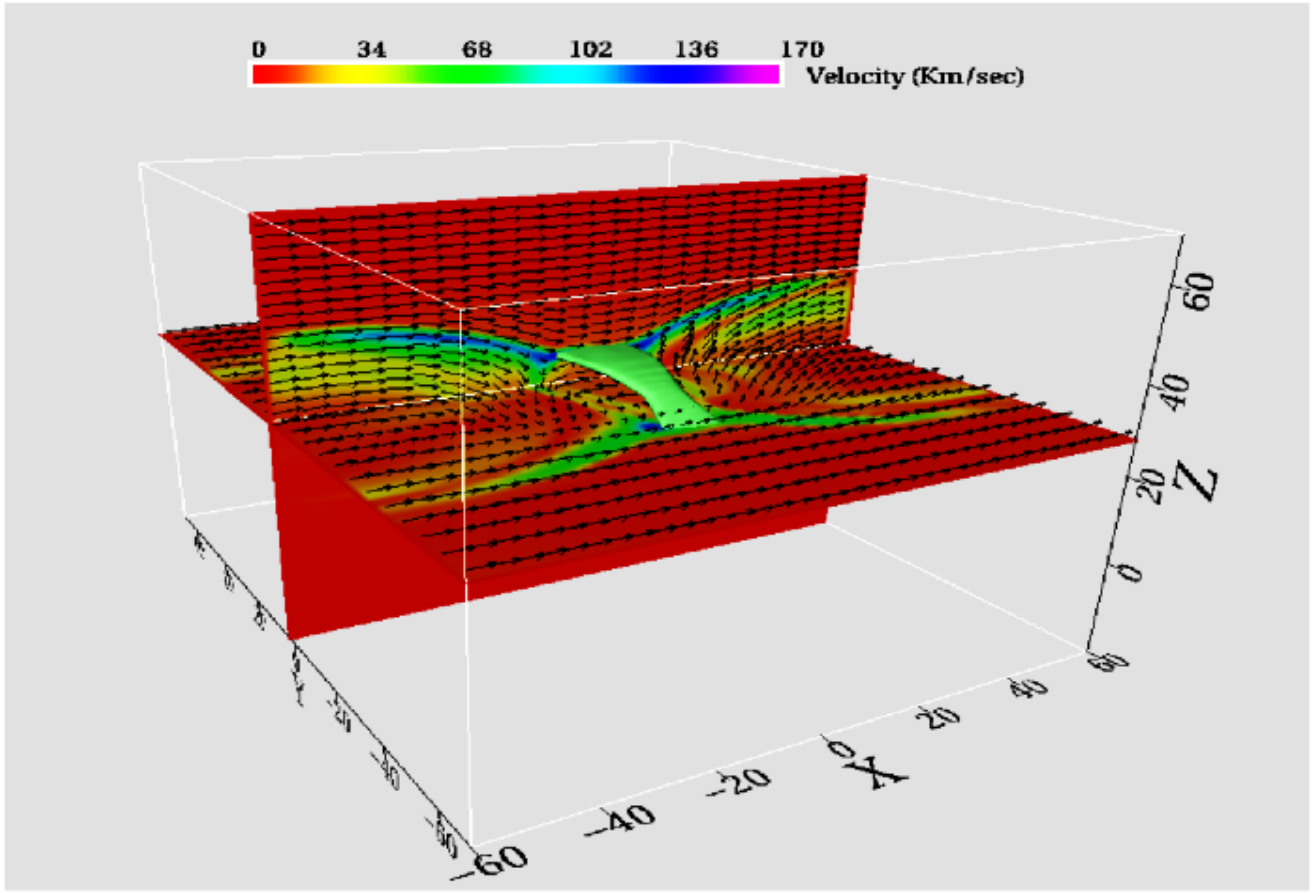

High-temperature reconnection jets

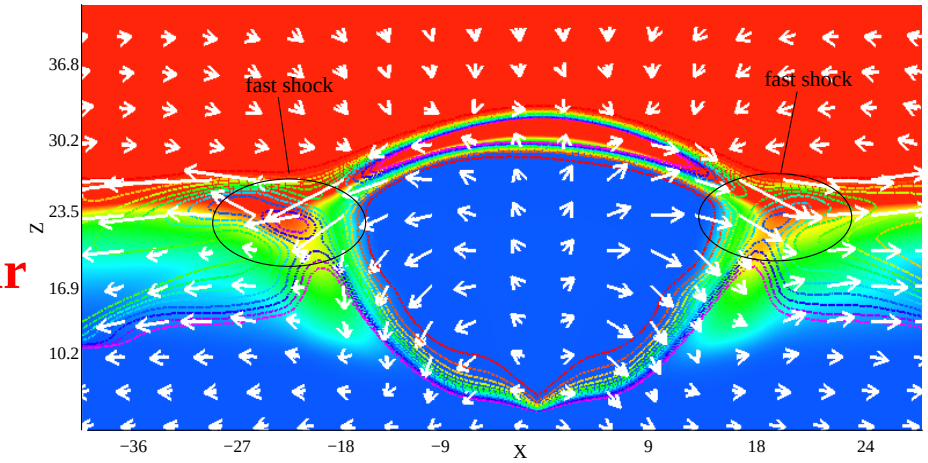

Acceleration mechanism similar to the 2D case of Yokoyama & Shibata (1996)

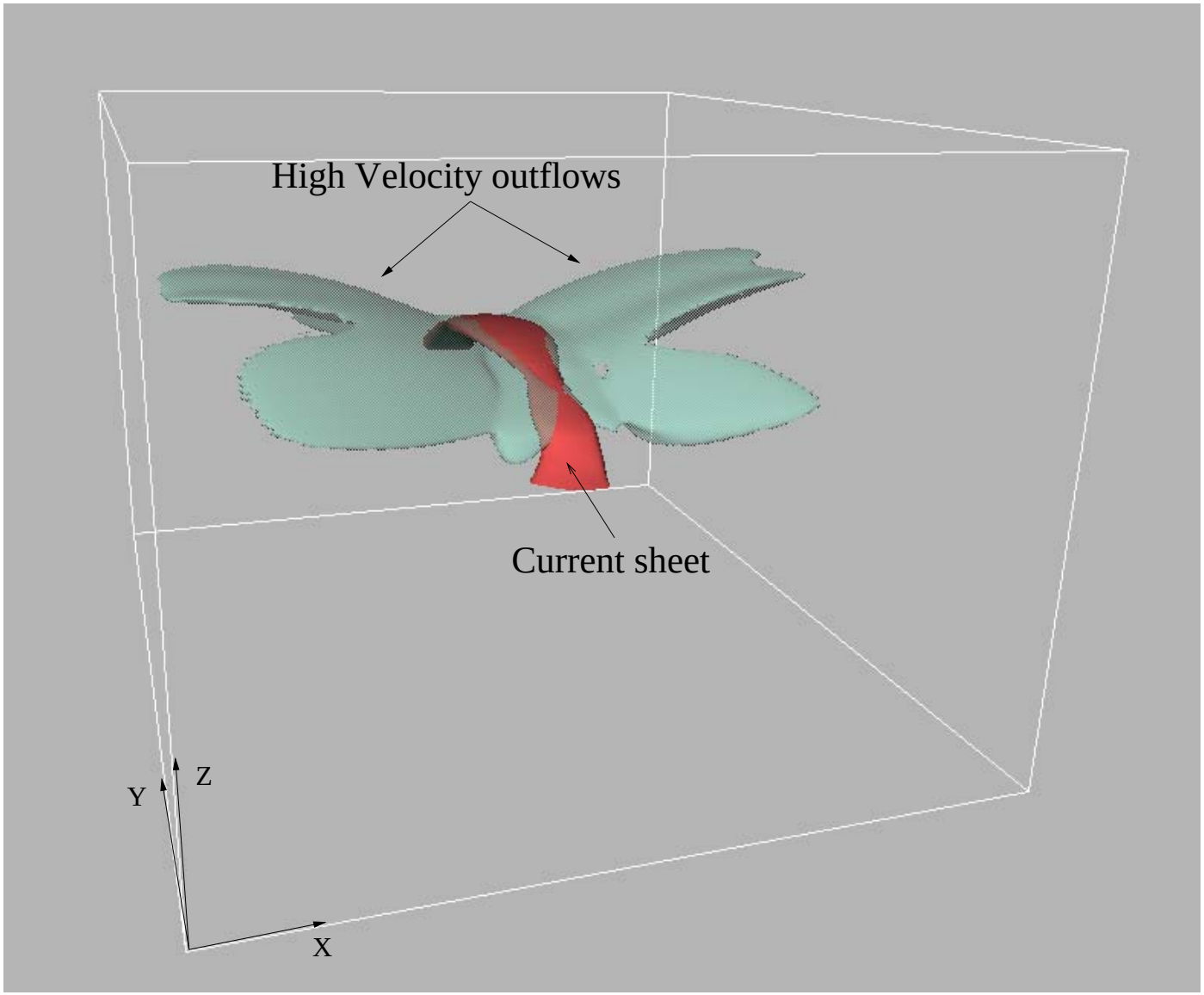
High Velocity outflows
Current sheet
Z
Y
X

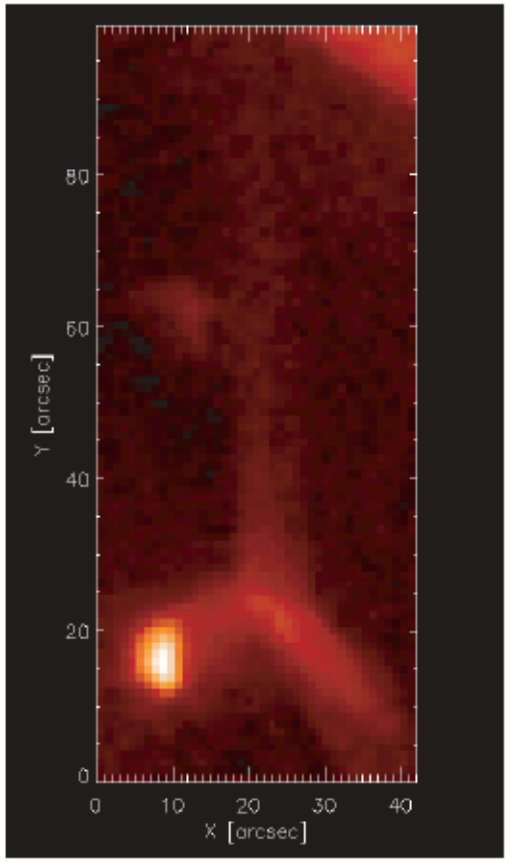

Fig. 1. Image of a polar coronal jet after the instrumental noise and cosmic particle hits had been removed. The image has also been normalized by exposure time and rotated vertically.

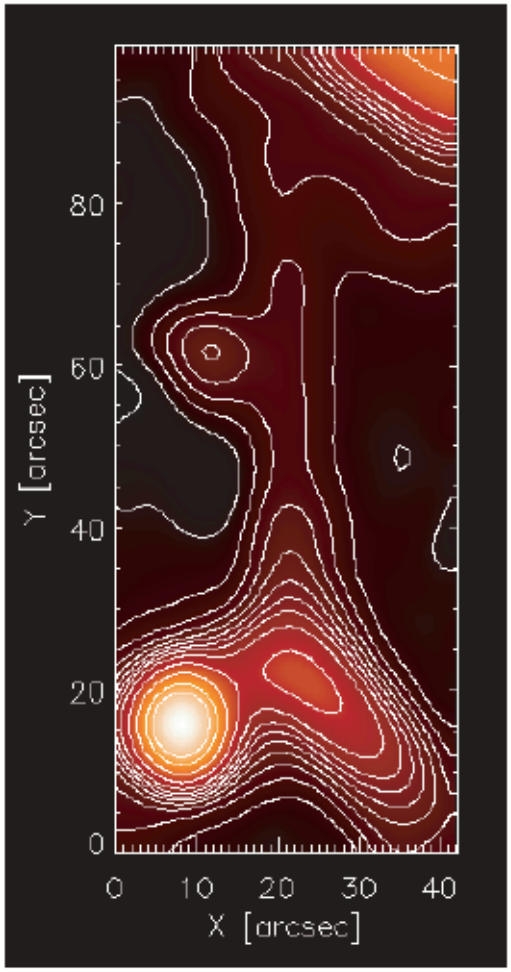

Fig. 2. Same image as shown in the previous figure after Gaussian low-pass and Laplacian edge-detection filters had been applied.

(Savcheva et al 2007)